Proceedings of the Korean Nuclear Society Autumn Meeting
Taejon, Korea, October 2000

An assessment methodology for in-vessel corium retention by external reactor vessel cooling during severe accidents in PWRs

Jae Hong Park

Korea Institute of Nuclear Safety,
19 Kusong-dong, Yusong-gu, Taejon, South Korea 305-338

Yong Hoon Jeong, Won-Pil Baek, and Soon Heung Chang

Department of Nuclear Engineering, Korea Advanced Institute of Science and Technology,
373-1 Kusong-dong, Yusong-gu, Taejon, South Korea 305-701

Abstract

A consistent probabilistic approach is proposed to evaluate the feasibility of in-vessel retention of the molten corium through external reactor vessel cooling (IVR-ERVC) during severe accidents of pressurized water reactors. By combining the results of Level-1 probabilistic safety assessment, a critical heat flux correlation, and wall heat flux distributions calculated by a severe accident code with appropriate adjustment, we can reasonably predict the overall success probability of the IVR-ERVC from the viewpoint of thermal failure. The practicability of the proposed approach is illustrated with a preliminary application to the Korean Standard Nuclear Power Plant. This paper also discusses future developmental needs for more reliable assessment.

Key words: in-vessel retention (IVR); external reactor vessel cooling (ERVC); severe accident; assessment methodology; critical heat flux (CHF)

1. Introduction

In-vessel retention (IVR) of a degraded core is considered as one of promising strategies for management of severe accidents in light water reactors (LWRs). The expected advantage of the IVR is to avoid various ex-vessel severe accident phenomena that are very complex and hard to resolve. One of applicable methods for IVR is the external cooling of the reactor pressure vessel by flooding the reactor cavity during severe accidents, i.e., in-vessel corium retention through external reactor vessel cooling (IVR-ERVC) [1, 2]. The IVR-ERVC concept as a severe accident management strategy has been applied to an existing LWR, i.e., the Loviisa plant of Finland [3] and to advanced PWR designs, i.e., the AP600 of USA [4] and Korean Next Generation Reactor (KNGR) [5]. This concept is also adopted in severe accident management guidelines of many existing reactors as a measure to slow down vessel failure [6].

The basic methodology for evaluating the performance of the IVR-ERVC for AP600 and Loviisa plants was the ROAAM (Risk-Oriented Accident Analysis Methodology) which was developed by Theofanous [7]. The ROAAM combines probabilistic methods, deterministic approaches and expert opinions in assessing risks of very low probability, high consequence situations. It resolves a safety issue involving complex phenomena by demonstrating that the associated risk is "physically unreasonable." The ROAAM has been utilized in resolving several safety issues, showing its usefulness as a novel safety assessment method.

The ROAAM has been successful in showing that there is a sufficient margin to failure when IVR-ERVC is applied to small-capacity LWRs such as AP600 (600 MWe) and Loviisa (465 MWe). However, direct application of the ROAAM becomes difficult for large-capacity LWRs with higher power density where the wall heat flux on the outer surface of the reactor vessel is expected to be high. This means that the general conclusion required by the ROAAM, "physically unreasonable," would be no longer valid for large reactors.

It is noted, however, that any single severe accident mitigation feature does not need to cover the whole severe accident scenarios. All the severe accident mitigation features and management strategies should be utilized together to minimize the risks to the public and environment in cases of unlikely severe accidents. In this sense, the IVR-ERVC can be adopted as one of severe accident mitigation features even for the large-capacity LWRs, and it may be necessary to determine the contribution of the IVR-ERVC rather than to strictly verify the complete coverage of all accident scenarios. This leads to a need for development of a methodology to determine the best-estimate success probability of the IVR-ERVC for large-capacity LWRs.

This paper proposes a consistent methodology to assess the success probability of the IVR-ERVC for specific reactor designs. The applicability of the methodology is illustrated with the Korean Standard Nuclear Power Plant (KSNP) design which is the CE type 1000 MWe pressurized water reactor (PWR) as an example. Future developmental needs for practical and reliable applications are also discussed.

2. Assessment Methodology

2.1. Basic assumptions and approaches

The objective of the proposed method is to determine the overall best-estimate success probability of the IVR-ERVC accident management strategy for possible core melt scenarios of PWR. The overall methodology was discussed by Baek et al. [8]. Important assumptions and approaches adopted in formulating the methodology are as follows:

(a) Utilize the core damage frequencies from the Level-1 probabilistic safety assessment (PSA) results combined with the depressurization probability after core melt;

(b) Assume "thermal failure" of the reactor vessel if the "wall heat flux (q''_{wall})" exceeds the "critical heat flux (CHF) (q''_{CHF})" on any location of the vessel external surface;

(c) Calculate the wall heat flux using integrated severe accident code calculations with

complementary calculations for obtaining limiting $q''_{wall}(q, t)$;

(d) Determine the critical heat flux on the external reactor vessel wall from available experimental data;

(e) Consider uncertainties in dealing with $q''_{wall}(q, t)$ and q''_{CHF}.

2.2. Assessment procedure

The overall procedure of the proposed methodology is illustrated in Fig. 1. Generally Steps 1 and 3 will be performed just once. However, Steps 2.1 through 2.4 should be repeated to every core melt scenario. In fact, the number of scenarios to be analyzed can be minimized by performing the analysis in the order from the severe and fast scenarios to moderate and slow ones.

Each step of the assessment procedure is discussed below.

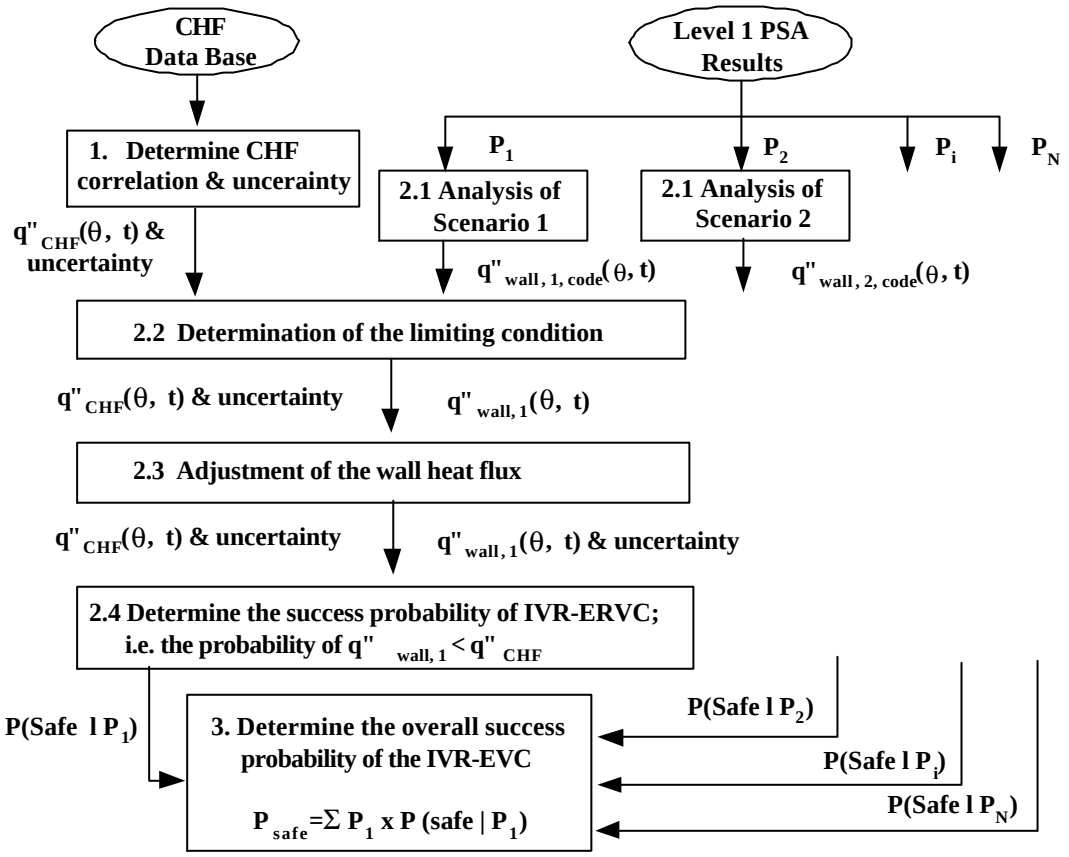

Fig. 1. Overall procedure of the proposed method

2.2.1. Step 1 - Determination of CHF correlation and uncertainty

A reliable prediction of the CHF on the reactor vessel external surface is very important for assessing the success probability of the IVR-ERVC. There are several relevant experimental works, the followings of which would be most relevant to the issue of IVR-ERVC:

- the ULPU series of experiment by Theofanous et al. [4, 9]

- the SBLB series of experiment by Cheung et al. [10, 11, 12]
- the SULTAN series of experiment by Rouge et al. [13, 14], and
- Russian work [15].

Now general trends of the CHF along the vessel surface and major parameters affecting the CHF have been identified. A conservative correlation can be developed from the experimental data as used in the assessments for AP600 and Loviisa. However, determination of a best-estimate (BE) correlation and its uncertainty for the application to the large-capacity reactor is not easy due to:

- CHF significantly depends on the specific channel and flow parameters; and
- Prototypic experimental simulation of a specific design would be very expensive.

However, it would be possible to develop a reasonable correlation and uncertainty by combining the presently available experimental data, analysis for expected flow conditions, and expert judgment. For a specific configuration, the CHF correlation may be simplified as a function of the location only, neglecting the change of flow conditions with time. The concept of CHF correlation and uncertainty is illustrated in Fig. 2(a).

2.2.2. Step 2 - Assessment of the success probability for a scenario

This step starts from the results of the Level-1 PSA for the specific plant. The Level-1 PSA provides the core damage scenarios and corresponding frequencies. In this paper, $P_1, P_2, \ldots, P_N$ are defined as the fraction of core damage frequency of scenarios *1*, *2*, …, *N*, respectively, to the total core damage frequency. Substeps 2.1-2.4 are explained for a specific Scenario *i*.

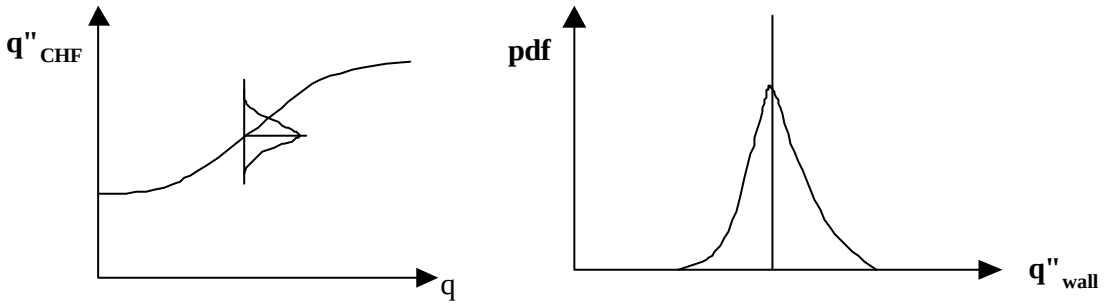

(a) CHF as a function of location and uncertainty distribution

(b) Wall heat flux distribution at limited location and time

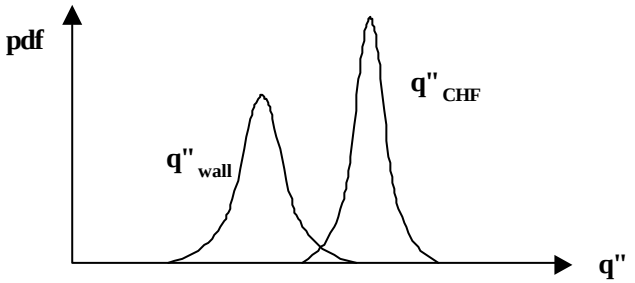

(b) Comparison of wall heat flux distribution with CHF distribution

Fig. 2. Illustration of work steps in the proposed methodology

Substep 2.1 - Analysis by a severe accident code

The thermal load on the reactor vessel lower head, i.e. the wall heat flux, depends on the accident scenario and varies with time and location. An integrated severe accident analysis code is used to adequately predict the time-dependent wall heat flux distributions for Scenario *i*, i.e. $q''_{wall,i,code}(\theta, t)$, where θ is the inclination angle of the surface in degrees ($\theta = 0°$ for the bottom of the lower head). It is possible to minimize the calculation efforts by performing the analysis from fast and severe scenarios with higher core damage frequency (CDF) contributions.

Substep 2.2 - Determination of the limiting condition

The limiting condition from the viewpoint of thermal failure can be determined by defining the location (θ) and time (t) where $q''_{wall,i,code}(\theta, t)/q''_{CHF}(\theta)$ becomes maximum. In this step, we can use the average values of heat fluxes with neglecting prediction uncertainties.

Substep 2.3 - Adjustment of the wall heat flux

The wall heat flux distributions calculated by the integrated code would not be sufficient for direct comparison with the CHF, owing to the limitation of presently available codes. They should be adjusted by incorporating the effects of focused heat flux in the metallic layer, coarse nodalization, simplified models and correlations, etc. by using the methodology developed by Theofanous et al. [4]. The adjusted wall heat flux distribution for the Scenario *i*, is denoted by $q''_{wall,i}(\theta, t)$. At this step, the uncertainties related to $q''_{wall,i}(\theta, t)$ can also be estimated by considering the uncertainties in the code models and thermophysical properties. Now we have q''_{CHF}, $q''_{wall,i}$, and their uncertainties for the limiting location and time. This step is illustrated in Figs. 2(b) and (c).

Substep 2.4 - Determination of the success probability of IVR-ERVC

In this step, the success probability of IVR-ERVC for the Scenario *i*, i.e. the probability of $q''_{wall,i} < q''_{CHF}$, is determined by comparing the distributions of wall heat flux with the critical heat flux at the limiting location and time. In general, numerical integration or Monte Carlo simulation can be used for this purpose. The calculated success probability for the Scenario *i* is denoted by $P(Safe|P_i)$. The probability distributions involved in this step is illustrated in Fig. 2(c).

2.2.3. Step 3 - Determination of the overall success probability of the IVR-ERVC

Finally, the overall success probability can be obtained by the weighted sum of the success probability for each scenario as follows:

$$P_{safe} = \sum_{i=1}^{N} P_i \cdot P(Safe \mid P_i) = \sum_{i=1}^{N} cdf_i \cdot P\left[q''_{wall,i}(\theta,t) < q''_{CHF}(\theta)\right] / \sum_{i=1}^{N} cdf_i \quad (1)$$

3. Preliminary Application to the KSNP Design

Application of the proposed methodology to a specific reactor design is not a simple task as it would require sufficient information and extensive analysis. However, the practicability can be verified through preliminary application to selected severe accident scenarios of the KSNP design which is a 1000 MWe PWR, as will be shown in this section. It should be noted that the assessment in this section is not a complete one but an illustration of the proposed methodology.

3.1. CHF correlation and uncertainty

It would be necessary to have CHF data from test facilities reliably simulating the KSNP design for reliable and accurate prediction of the CHF. However, with regard to the CHF correlation and uncertainties, it is believed that a reasonable correlation can be developed by fully utilizing the presently available information as discussed by Yang et al. [16].

The KSNP reactor has 45 instrument penetrations with diameter of 0.0762 m through the hemispherical lower head of the reactor vessel. The reactor vessel is enclosed with the stainless steel thermal insulator. A natural circulation flow path would be established through the annular gap between the reactor vessel and the thermal insulator when the reactor cavity is flooded to a sufficiently high level. Among various CHF tests, it is preliminarily concluded that ULPU Configuration II tests under natural circulation (~120 gpm and ~130 gpm) [4, 17] would be the most appropriate for simulation of the KSNP reactor design.

In this study, for illustration of the proposed methodology, a CHF correlation is developed from 50 CHF data of Theofanous et al. [4, 17]:

$$q''_{CHF}(q) = 536.5 + 18.997q - 0.108q^2 - 6.37\text{x}10^{-4}\, q^3 + 8.51\text{x}10^{-6}\, q^4 \quad \text{kW/m}^2 \qquad (2)$$

The standard deviation of the prediction error is 82.1 kW/m^2; a normal distribution is assumed for the purpose of this preliminary assessment. Fig. 3 compares the developed CHF correlation with experimental data.

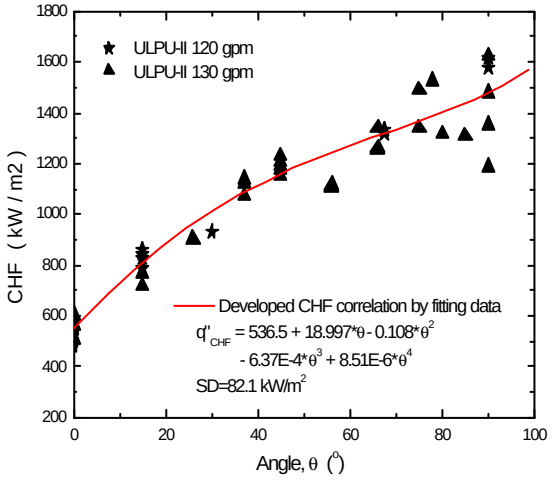

Fig. 3 The CHF correlation and experimental data

3.2. Assessment of success probabilities for selected scenarios

The result of the level 1 PSA for a KSNP, Ulchin Units 3&4 [18], is summarized in Table 1. Total core damage frequency (CDF) of Ulchin Units 3&4 is evaluated to be 8.25×10^{-6}/yr. The IVR-ERVC is applicable to low-pressure core damage scenarios, such as large-, medium-, and small-break loss-of-coolant accidents (LOCAs). It is also applicable to most of high-pressure core damage scenarios, as depressurization process would be initiated after detection of core melt and core damage would progress at low pressures.

Each scenario shown in Table 1 consists of several sub-scenarios. Therefore, total number of scenarios to be considered is several times of that shown in the table. However, the number of scenarios, for which actual analysis is required, can be significantly reduced by clustering similar scenarios and by performing the analysis from fast scenarios.

For illustration of the proposed methodology, we select 3 LOCA sub-scenarios for further analysis:

- LL-5 representing the large-break LOCAs with CDF fraction of 12.7%
- ML-3 representing the medium-break LOCAs with CDF fraction of 7.7%
- SL-9 representing the small-break LOCAs with CDF fraction of 22.5%

Table 1. Summary of Level-1 PSA results for a KSNP

Core Damage Scenarios	CDF/yr	% CDF
Large-break LOCAs	1.05E-6	12.7
Medium-break LOCAs	6.33E-7	7.7
Small-break LOCAs	1.86E-6	22.5
SGTR	1.14E-6	13.8
Large Secondary Side Break	1.46E-7	1.8
Loss of Main Feedwater	1.14E-6	13.8
Loss of Condenser Vacuum	2.53E-8	0.3
Loss of a CCW train	1.25E-7	1.5
Loss of a 4.16KV AC bus	5.48E-10	< 0.1
Loss of a 125V DC bus	3.17E-7	3.8
Loss of Off-site Power	3.97E-7	4.8
Station Blackout	4.80E-7	5.8
General Transients	3.59E-7	4.4
ATWS	3.15E-7	3.8
Interfacing System LOCA	1.77E-9	< 0.1
Reactor Vessel Rupture	2.66E-7	3.2
Total CDF	8.25E-6	100.0

3.2.1. Analysis of scenarios by a severe accident code

For the wall heat flux calculation, an integrated system code, MAAP 4, is used because it is presently available, fast-running, and relatively robust. More detailed codes such as MELCOR may be used to complement the fast-running code. The MAAP 4 code divides the lower head of

the reactor vessel into 5 nodes and calculates the average heat flux for each node. The node 1 is from 0° (the bottom of lower head) to 18° and node 5 is from 72° to 90°. The KSNP has about 86 tons of UO_2 and 24 tons of Zr. The available stainless steel mass that can be melted and relocated into the lower plenum is about 33 tons. The MAAP code calculates the decrease of decay heat power level for the relocated core materials with reflecting the escape of noble gases and volatile fission products. Fig. 4 illustrates the calculated change of wall heat fluxes with time for LL-5.

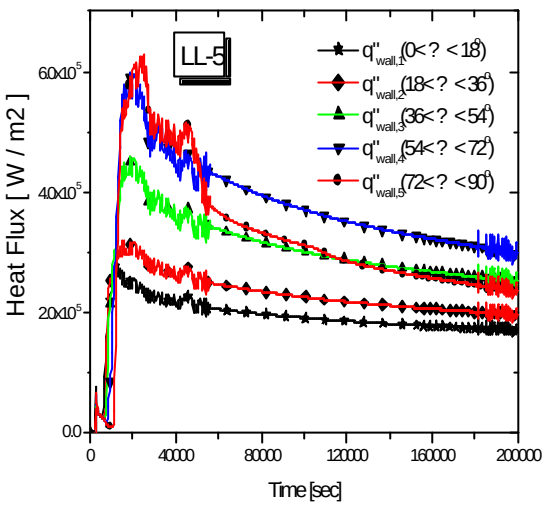

Fig. 4 Calculated wall heat fluxes for LL-5

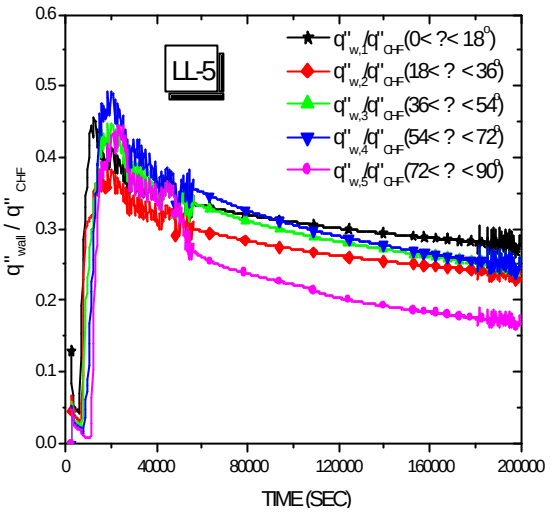

Fig. 5 Determination of limiting condition for LL-5

3.2.2. Determination of limiting conditions

The limiting condition from the view point of thermal failure is determined by the location and time where $q''_{wall,i,code}(q, t) / q''_{CHF}(q)$ becomes maximum as described in Section 2.2.2 (see Fig. 5). The validity of the calculated results and the uncertainties in the wall heat flux and CHF are not strictly considered in this preliminary assessment. The calculated limiting conditions are summarized in Table 2.

Table 2. Important parameters at limiting conditions of LL-5, ML-3 and SL-9 scenarios

Analysis case	% of total CDF	Limiting condition				Relocated mass in lower plenum, ton	
		time, s	$q''_{wall,i,code}$, kW/m^2	$q''_{wall,i,code}(\theta, t) / q''_{CHF}(\theta)$	decay power, MW	oxide	metal
LL-5	5.84	18,590	598.4	0.493	20.09	108.2	28.21
ML-3	2.45	64,940	398.4	0.390	13.55	105.3	22.33
SL-9	13.45	66,010	407.8	0.336	14.07	108.0	28.19

3.2.3. Adjustment of limiting heat fluxes by complementary calculations

The wall heat fluxes calculated by MAAP 4, $q''_{wall,i,code}(q, t)$, are adjusted to obtain the limiting wall heat flux by complementary calculation based on the methodology developed by Theofanous et al. [4]. In the hemispherical lower head of a reactor vessel, a relatively thin metal layer is assumed to overlie the oxide pool. Assuming the steady-state condition under natural convection, the overall energy balance model on the oxide pool is used to determine the average upward and downward heat fluxes. The 3-dimensional 1/2 scale experiment by Theofanous et al. [17], ACOPO, and 2-dimensional full scale experiment by Bernaz et al. [19], BALI, are large scale tests performed to simulate the natural convection heat transfer from volumetrically heated pools of hemispherical geometry. In this work, the results of BALI experiment are used to determine the average upward and downward heat fluxes because they lead to the higher wall heat fluxes in the metallic layer.

The wall heat flux distribution as function of the lower head inclination angle in the oxide pool is evaluated by the correlation obtained from the mini-ACOPO data [4]. The wall heat flux in the metal layer is determined by considering the balance between the heat input from the oxide pool and heat losses to the upper structures and the side wall. With introducing some simplifying assumtions, the wall heat flux to CHF ratio can be calculated as shown in Fig. 6.

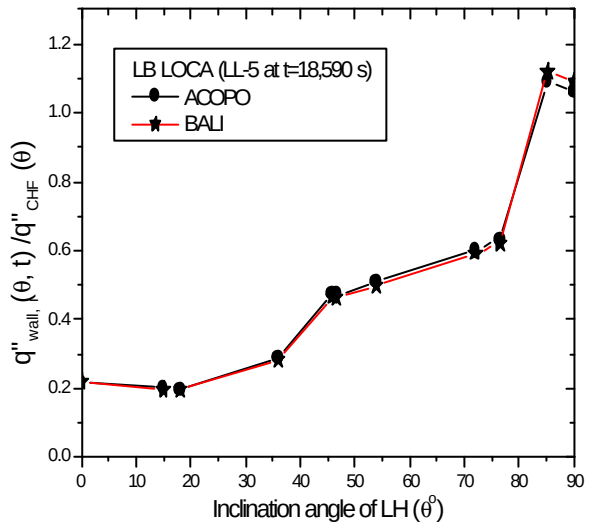

Fig. 6 Adjusted wall heat flux divided by the CHF for LL-5

It can be noted from Fig. 6 that the wall heat flux increases sharply and becomes limiting in the metallic layer region overlying the oxide melt pool. The wall heat flux in the metallic layer depends on the melting temperature which is basically determined by the mole fraction of zirconium. It is noted that the melting temperature and consequent wall heat flux of the metallic layer are subject to probability distributions due to the insufficient state of knowledge. If the Zr oxidation fractions are in the range of 40 to 75% of total Zr (24 ton), the corresponding zirconium fractions of the metallic layer indicate the range of melting temperature between 1,680 to 1,920 K

based on the iron-zirconium phase diagram by Pelton et al. [20]. As the lower melting temperature of metallic layer results in the higher sidewall heat flux, we conservatively assumed a uniform distribution of melting temperature between 1600 to 1700 K. This idea is illustrated in Fig. 7.

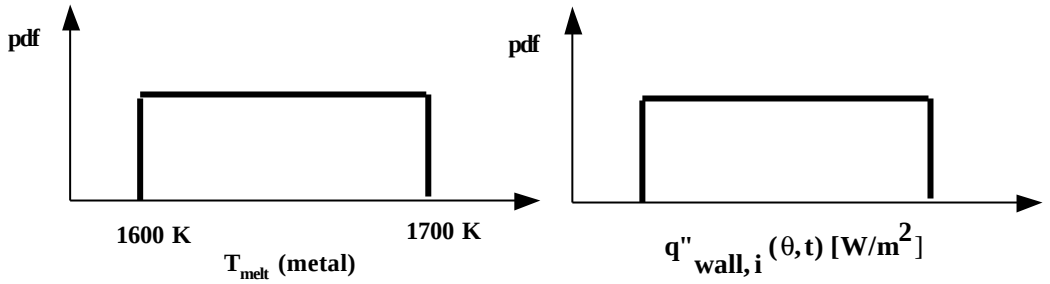

Fig. 7 Adjusted wall heat flux distribution for Scenario i

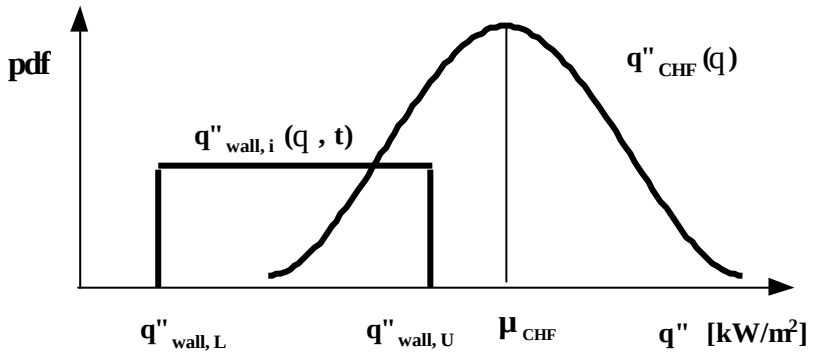

Fig. 8. Estimation of the IVR-ERVC success probability for a scenario

3.2.4. Determination of success probability for each scenario

The success probability of each scenario, i.e., $P(safe|P_i)$ = Probability $[q''_{wall,i} < q''_{CHF}]$, can be calculated by applying Monte Carlo simulation to the wall heat flux with uniform distribution and the CHF with normal distribution. The concept is illustrated in Fig. 8 and the calculated results are summarized in Table 3. It is shown that the success probability of the IVR-ERVC is 100%, near 100% and negligible for small-break, medium-break, and large-break LOCAs, respectively.

Table 3. Success probabilities for scenarios LL-5, ML-3, SL-9

Scenario	Metallic layer		CHF, kW/m^2	P(safe|P$_i$) = P (q"$_w$ < q"$_{CHF}$)
	T $_{melt}$, K	q"$_{wall,i}$, kW/m^2		
LL-5 at 18,590s	1,600	1,774	m = 1,393 (s = 82.1)	0.015%
	1,700	1,598		

ML-3 at 64,940s	1,600	1,269	m = 1,383 (s = 82.1)	98.4%
	1,700	1,073		
SL-9 at 66,010s	1,600	1,161	m = 1,395 (s = 82.1)	100%
	1,700	1,000		

3.2.5. Overall success probability

The overall success probability can be estimated by Eq. (1) after success probabilities are also assessed for other scenarios. Some scenarios require the calculation process shown in the preceding sections; but others including scenarios faster than LL-5 or slower than SL-9 may by judged by simple considerations.

The process of calculating the overall success probability is illustrated in Table 4. 30.10% in Table 4 represents 70% of the CDF fraction of LOCA scenarios (42.95%), that is, the success probability of the IVR-ERVC is assessed to be 70% for LOCAs. The overall success probability for all scenarios can be determined after performing further analysis. The symbol A in Table 5 represents the success probability that will be added by other scenarios.

Table 4. Overall success probability of IVR-ERVC

Scenario	CDF_i /yr	$P_i = CDF_i / \Sigma CDF$	$P(safe\|P_i) = P(q"_w < q"_{CHF})$	$P_i \times P(safe\|P_i)$
LB LOCA	1.05E-06	12.73%	0.015%	0.0019%
MB LOCA	6.33E-07	7.67%	98.4%	7.55%
SB LOCA	1.86E-06	22.55%	100%	22.55%
. . .	. . .	. . .	. . .	a_1
. . .	. . .	. . .	. . .	. . .
. . .	. . .	. . .	. . .	a_n
		$\Sigma P_i \times P(safe\|P_i) = \Sigma CDF_i \times P(q"_w < q"_{CHF}) / \Sigma CDF_i =$		30.10% + A[a]

[a] $A = a_1 + a_2 + a_3 + \ldots + a_n$

3.2.6. Discussions

It should be noted that the preliminary application in this paper is just to show the practicability of the proposed methodology. However, the present analysis has also provided the approximate values of success probability for LOCA scenarios. More LOCA scenarios may also be analyzed to obtain more accurate success probability.

There are several works to be done in order to obtain a reliable success probability of the IVR-ERVC for the KSNP. One of important tasks is to develop a CHF correlation that properly incorporates the design characteristics of the KSNP. Another important parameter is the possibility of successful depressurization after the onset of core damage for high-pressure core melt scenarios as the overall success probability significantly depends on this depressurization process. Further refinement on the process of calculating wall heat flux distributions is also important. In particular, more improvement would be possible for the severe accident analysis by an integrated code and the

treatment of the focused heat flux in the metallic layer. The integrity of instrument penetrations, although which is not addressed in here, should be evaluated adequately. Regardless of various limitations, however, it is believed that the preliminary application to the KSNP has illustrated the assessment procedure and verified the practicability.

If the calculated success probability of the IVR-ERVC is not sufficiently high, the effects of vessel failure and other mitigation features should be considered together in assessing the overall capability of severe accident mitigation.

4. Conclusions

This paper proposes a new probabilistic approach to evaluate the feasibility of the IVR-ERVC during severe accidents of PWRs. The following conclusions can be drawn from this work:

(a) A consistent approach to evaluate the best-estimate success probability of the IVR-ERVC for PWRs from the viewpoint of thermal failure can be established by combining the results of Level-1 probabilistic safety assessment, a critical heat flux correlation, and wall heat flux distributions calculated by a severe accident code with appropriate adjustment.

(b) A preliminary application to the KSNP design has demonstrated the practicability of the proposed approach for specific reactor designs.

(c) A further refinement of the procedure would be possible in actual applications, including an improved CHF correlation, more reliable severe accident analysis, more reliable adjustment of the wall heat flux, etc.

Acknowledgment

This work was performed under the financial support of Ministry of Science and Technology of Korean Government.

References

1. Henry R.E. and Fauske K. "External Cooling of Reactor Vessel Lower Head Under Severe Accident Conditions," Nucl. Eng. Des., 64, 433-445, 1993
2. Theofanous T.G., "In-Vessel Retention As a Severe Accident Management Strategy, Proc. OECD/NEA/CSNI Workshop on In-Vessel Core Debris Retention and Coolability," Mar. 3-6, 1998. Garching, Germany.
3. Kymäläinen O., Tuomisto H., Theofanous T.G., "In-Vessel retention of corium at the Loviisa plant," Nucl. Eng. Des., 169, 109-130, 1997.
4. Theofanous T.G. et al., "In-Vessel Coolability and Retention of a Core Melt," DOE/ID-10406, Vols. 1 & 2, 1996.
5. Oh S.J., "The Role of IVR from the Severe Accident Management Perspective, Proc. Workshop on In-Vessel Retention for the KNGR Severe Accident Management," Aug. 27, 1999, KEPRI,

Taejon, Korea.
6. KAERI (Korea Atomoic Energy Research Institute), "Development of Accident Management Guidance for Korean Standard Nuclear Power Plant," KAERI/RR-1939/98, 1999.
7. Theofanous T.G., "On the Proper Formulation of Safety Goals and Assessment of Safety Margins for Rare and High-Consequence Hazards," Reliability Eng. & System Safety, 54, 243-257, 1996.
8. Baek W.P, Chang S.H, and Park J.H, "A Proposed Methodology for Assessment of External Vessel Cooling During Severe Accidents in Pressurized Water Reactors," Proc. KNS Autumn Meeting, Seoul, 1999.
9. Theofanous T.G. and Syri S., "The coolability limits of a reactor pressure vessel lower head," Nucl. Eng. Des., 169, 59-76, 1997.
10. Cheung F.B., Haddad K. H. and Liu Y.C., "Critical Heat Flux (CHF) Phenomenon on downward Facing Curved Surface," NUREG/CR-6507, 1997.
11. Cheung F.B. and Liu Y.C., "Critical Heat Flux (CHF) Phenomenon on a Downward Facing Curved Surface: Effects of Thermal Insulation," NUREG/CR-5534, 1998.
12. Cheung F.B. and Liu Y.C., "CHF Experiments to Support In-Vessel Retention Feasibility Study For an Evolutionary ALWR Design," Preliminary Final Project Report, EPRI WO# 5491-01, 1999.
13. Rouge S., "SULTAN Test Facility for Large Scale Vessel Coolability in Natural Convection at Low Pressure," Nucl. Eng. Des., 169, 185-195, 1997.
14. Rouge S., and Geffraye G., "Reactor Vessel External Cooling for Corium Retention SULTAN Experimental Program and Modelling with CATHARE Code," Proc. OECD/NEA/CSNI Workshop on In-Vessel Core Debris Retention and Coolability, March 3-6, 1998, Garching, Germany.
15. Granovskiy V.S. et al., "An Experimental Study of the CHF at the External Cooling of Reactor Vessel," Proc. Thermophysics-90 (Russian), 1995.
16. Yang S.H., Baek W.P. and Chang S.H., "An Analysis of Critical Heat Flux on the External Surface of the Reactor Vessel Lower Head," Proc. KNS Autumn Meeting, Seoul, 1999.
17. Theofanous T.G. et al., "The first results from the ACOPO experiment, Nucl. Eng. Des.," 169, 49-57, 1997.
18. KEPCO (Korea Electric Power Corporation), "Ulchin units 3&4, Final Probabilistic Safety Assessment Report," rev. 1, 1998.
19. Bernaz L. et al., "Thermal hydraulic Phenomena in Corium Pools: Numerical Simulation with TOLBIAC and Experimental Validation with BALI," Proc. OECD/ NEA/CSNI Workshop on In-Vessel Core Debris Retention and Coolability, March 3-6, 1998, Garching, Germany.
20. Pelton, A.D. et al., "Thermodynamic Analysis of Phase-Equilibria in the Iron Uranium Zirconium System," J. Nucl. Materials, 210(3), 324-332, 1994.